A Parcel-Scale Coastal Flood Forecasting Prototype for a Southern California Urbanized Embayment

Authors: Gallien, Timu W., Barnard, Patrick L., van Ormondt, Maarten, Foxgrover, Amy C., and Sanders, Brett F.

Source: Journal of Coastal Research, 29(3) : 642-656

Published By: Coastal Education and Research Foundation

URL: https://doi.org/10.2112/JCOASTRES-D-12-00114.1

Journal of Coastal Research	29	3	642–656	Coconut Creek, Florida	May 2013

A Parcel-Scale Coastal Flood Forecasting Prototype for a Southern California Urbanized Embayment

Timu W. Gallien[†], Patrick L. Barnard[‡], Maarten van Ormondt[§], Amy C. Foxgrover[‡], and Brett F. Sanders[†]

[†]Civil and Environmental Engineering
University of California, Irvine
Irvine, CA 92697, U.S.A.

[‡]Pacific Coastal and Marine Science Center
United States Geological Survey
Santa Cruz, CA 95060, U.S.A.

[§]Deltares
P.O. Box 177
2600 MH, Delft, The Netherlands

www.cerf-jcr.org

www.JCRonline.org

ABSTRACT

Gallien, T.W.; Barnard, P.L.; van Ormondt, M.; Foxgrover, A.C., and Sanders, B.F., 2013. A parcel-scale coastal flood forecasting prototype for a Southern California urbanized embayment. *Journal of Coastal Research,* 29(3), 642–656. Coconut Creek (Florida), ISSN 0749-0208.

Coastal flood risk in California is concentrated around urbanized embayments that are protected by infrastructure, such as levees, pumps, and flood walls, which pose a challenge to accurate flood prediction. A capability to predict coastal urban flooding at the parcel-scale (individual home or street) from high ocean levels (extreme high tides) is shown here by coupling a regional ocean forecasting system to an embayment-scale hydrodynamic model that incorporates detailed information about flood defenses. A unique flooding data set affords the rare opportunity to validate model predictions and allows us to identify model data that are essential for accurate forecasting. In particular, results show that flood defense height data are critical, and here, that information is supplied by a Real Time Kinematic Global Positioning System (RTK-GPS) survey, which yields *ca*. 1-cm, vertical root mean-squared error accuracy. Bathymetry surveys and aerial Light Detection and Ranging (LIDAR) data characterizing the embayment also prove essential. Moreover, hydrodynamic modeling of flood inundation is shown to significantly improve on planar surface models, which overestimate inundation, particularly when manipulated to account for run-up in a simplistic way. This is attributed to the transient nature of overtopping flows and motivates the need for dynamic, spatially-distributed overtopping models that are tailored to the urban environment.

ADDITIONAL INDEX WORDS: *Inundation, sea level rise, storm surge, validation, urban coastal flooding, CoSMoS, multiscale model, regional model, DEM, DTM, flood risk, coastal hazard.*

INTRODUCTION

Coastal flooding represents a significant socioeconomic and humanitarian threat to urbanized lowlands throughout the world. Currently, 20 million people worldwide live below high tide (Nicholls, 2011). Globally, sea levels are projected to rise on the order of 1 m during the 21st century (Vermeer and Rahmstorf, 2009), and multimeter sea-level rise is expected in the next several centuries (Jevrejeva, Moore, and Grinsted, 2012). In the United States, more than 125,000 km^2 and almost 25 million people are located in census block groups that border the open ocean (Crowell *et al.,* 2010). Similarly, California coastal sea levels are projected to rise 1–1.4 m in the next century (Cayan *et al.,* 2009), and evidence indicates mean tidal ranges and, consequently, mean higher high water (MHHW) may be increasing more rapidly than mean sea level in areas of the Southern California Bight (Flick, Murray, and Ewing, 2003). Furthermore, Bromirski *et al*. (2011) show that quasi-cyclical wind-stress patterns in the eastern North Pacific have suppressed sea-level rise rates along the West Coast since 1980, and a pending reversal in this pattern would result in the resumption of regional sea-level rise rates equivalent to, or exceeding, global mean sea-level rise rates. Topographic sea-level rise vulnerability analysis conducted by Strauss *et al*. (2012) demonstrates more than 325,000 Californians are already living within 1 m of local-mean high water and a statewide impact assessment indicates approximately one-quarter of a million residents are currently exposed to a 100-year coastal flood (Heberger *et al.,* 2009). Alarmingly, Tebaldi, Strauss, and Zervas, (2012) suggest the current 100-year coastal flooding event will recur yearly by 2050 in Southern California. Collectively, these studies demonstrate the exceptional vulnerability of urbanized embayments in general, and Southern California in particular, to future impacts associated with coastal flooding.

Flood mitigation strategies (or adaptation strategies in the context of climate change) offer the potential for substantial benefits and include early warning systems, upgraded protection, subsidence management, building regulation and retrofitting, land use planning, selective relocation, and risk sharing through insurance (Hanson *et al.,* 2011). To identify the best mix of measures for a particular area, the investment cost of each option can be weighed against benefits defined by avoided damages, and returns on the order of four to one have been reported (MMC, 2005). Damages are estimated by combining

DOI: 10.2112/JCOASTRES-D-12-00114.1 received 31 July 2012; accepted in revision 2 August 2012; corrected proofs received 9 October 2012.
Published Pre-print online 6 November 2012.

asset data with flood intensity and duration data computed with flood inundation models and by studying business interruptions that result in a loss of commerce. Flood modeling is focused not only on present-day flood intensities (*i.e.,* depth, velocity) from chosen flood scenarios (*e.g.,* 100-year event) but also on future intensities considering climate changes (*e.g.,* higher sea level, surges, waves, and increased runoff) and also the effect of mitigation measures (*e.g.,* flood defense and land use changes). Hence, models must be sensitive to changes in infrastructure and land uses. Flood mapping also plays an important role in early warning systems and emergency management, but in this case, the goal is to simulate a specific event instead of a design scenario. Early warning systems can yield remarkable benefits in terms of damages avoided. Studies have shown that with several hours warning, flood losses can be reduced by as much as 50% (Smith, 1994). However, early warning efficacy hinges on reliable flood forecasting because public cooperation may diminish following false alarms.

On the U.S. West Coast, prediction of episodic flooding events requires simulation of a suite of physical processes that include atmospheric forcing, tides, storm surge, nearshore wave transformation, wave setup, wave run-up, flood wall overtopping, and overland flow. Existing literature presents an effective modeling methodology for simulating the effects of cyclones and large storms in nearshore waters (*e.g.,* Brown, Spencer, and Moeller, 2007; Bunya *et al.,* 2010; Mulligan *et al.,* 2011; Padilla-Hernandez *et al.,* 2007; Sheng, Alymov, and Paramygin, 2010; Sheng, Zhang, and Paramygin, 2010). These large-scale simulations rely on atmospheric forcing, either modeled or empirically hindcast, coupled to a global spectral wave model, such as WAM (Hasselman *et al.,* 1998) or WAVEWATCH III (Tolman, 1997), which informs a regional wave model, such as SWAN (Holthuijsen, Booji, and Ris, 1993), to resolve nearshore wave transformation. In the United States, the National Oceanic and Atmospheric Administration (NOAA) operates hurricane storm-surge forecasts using the SLOSH model (Jelenianski, Chen and Shaffer, 1992) over large areas of the Gulf and Atlantic Coasts, Hawaii, Puerto Rico, the U.S. Virgin Islands, and the Bahamas. The United Kingdom's Environment Agency manages a comprehensive, online flood-management program issuing 3-day forecasts for the entirety of the United Kingdom. In 2007, the European Commission issued the European Flood Directive, which requires all member states to identify riverine and coastal areas at risk by 2011, produce flood maps by 2013 and develop prevention, protection, and preparedness plans by 2015 (European Commission, 2012). In Southern California, considerable effort has been focused on the development of operational nowcast and forecast systems, including the Scripps Institute of Oceanography Coastal Data Information Program (CDIP), which focuses primarily on wave predictions (O'Reilly and Guza, 1993; O'Reilly *et al.,* 1993) and the United States Geological Survey (USGS) Coastal Storm Modeling System (CoSMoS: Barnard *et al.,* 2009).

CosMoS was developed by the USGS in collaboration with Deltares, Scripps Institution of Oceanography, Oregon State University, University of Florida, and the National Park Service, for assessing the physical effects of powerful storms, with both real-time and offline applications. CoSMoS is being applied operationally and offline to the Southern California region (Point Conception, California, to the Mexican Border) (http://cosmos.deltares.nl/SoCalCoastalHazards/index.html) for hindcasts and for assessing the impact of future storms influenced by sea-level rise and climate change. CoSMoS applies a predominantly deterministic framework to make predictions of coastal inundation, flooding, erosion, and cliff failures. The model integrates atmospheric-forcing information from the NOAA Global Forecast System (GFS) with a global wave model, WaveWatch III, and suite of physical-process models for tide, surge, and waves to predict currents, water level, wave conditions, wave run-up, and shoreline change. The output includes predictions of nearshore water levels, wave climate, and sediment transport with a resolution of approximately 100 m alongshore. Flooding projections are then made by Planar Surface Projection (PSP) of water levels onto a 3-m spatial resolution digital elevation model (DEM) assembled from a variety of sources with vertical accuracies that vary from decimeters to meters (Barnard and Hoover, 2010).

The PSP (also known as the *bathtub* or *equilibrium*) model is unreliable in urbanized lowlands protected by defenses because flood extent is a result of the volume of flood water that penetrates defenses, not the water level itself (Bates *et al.,* 2005; Gallien, Schubert, and Sanders, 2011). This volume is controlled by the height and duration over which water penetrates low or weak points in flood defenses and because flood events rarely last sufficiently long for water heights on both sides of defenses to equilibrate, these models tend to significantly overestimate flood effects (Bates *et al.,* 2005, Gallien, Schubert, and Sanders, 2011). In limited cases, raster-based models have accounted for fine-scale hydraulic structures, such as dikes or ditches, by setting pixel elevation to wall heights (*e.g.,* Poulter and Halpin, 2008), but this alone does not impart an ability to predict overtopping volumes. Attention must, therefore, be focused on models that account for key processes, including dynamic overtopping flows caused by high water levels and/or waves, overland flow, and potentially subsurface (*i.e.,* sewer) flows. Regional modeling systems, such as CoSMoS, can be applied with increasing resolution and higher-quality topographic data to resolve the processes that contribute to lowland flooding, but the computational demands required to resolve hydraulically important urban features, such as walls, wharves, and streets (*ca*. 3 m), conflict with the need for efficient modeling at the regional scale (Sanders Schubert, and Detwiler, 2010). This can be overcome with super-computing resources, but regional modelers still face a major challenge accessing data with the resolution and accuracy required for parcel-scale (individual home or street) flood prediction. For example, Strauss *et al*. (2012) were limited by a *ca*. 1-m vertical accuracy DEM in studying sea-level rise effects across the continental United States. Multiple studies have shown the importance of fine-scale topographic data for flood prediction (Néelz *et al.,* 2006; Poulter and Halpin, 2008; Webster *et al.,* 2004), but such data are typically managed by local authorities and may not be available for public dissemination. Even in cases where aerial Light Detection and Ranging (LIDAR) data exist (typically 10–15 cm vertical accuracy), Gallien, Schubert, and Sanders (2011) show that flood defenses need to be carefully inspected at the local level to

identify vulnerabilities in flood defenses, flood walls, and embankments and must be accurately surveyed with *ca*. 1-cm vertical accuracy to predict the onset of overtopping. Moreover, carefully processed, aerial LIDAR data are needed to resolve overland flow, and accurate bathymetry data are needed to account for tidal amplification within coastal embayments (Gallien, Schubert, and Sanders 2011). Considering the number of localized embayments (*e.g.,* Marina del Rey, Huntington Harbor, Newport Bay, Mission Bay, and San Diego Bay, California) that can be found within a regional domain, such as the Southern California Bight, it becomes clear that the tasks of data collection and model verification are daunting at the regional scale.

This article presents a prototype for parcel-scale, urban flood prediction: regional model support of a local model. That is, we argue that the embayment scale is the appropriate extent for a local hydrodynamic inundation model supported by local data and site knowledge, which relies on a regional model for external forcing, including predictions of ocean water levels and waves and that can readily support a local decision-making process. Additional motivation is provided by a relatively simple, one-way coupling of regional and local models. Here, we focus on Newport Bay, California, where the BreZo hydrodynamic model (Begnudelli, Sanders, and Bradford, 2008; Sanders, 2008) has been validated for parcel-resolution flooding predictions driven by high water levels (Gallien, Schubert, and Sanders, 2011). This serves as the local model, and CoSMoS is used for regional modeling based on its track record for support of coastal-hazards prediction in Southern California (Barnard *et al.,* 2009). Thus, CoSMoS and BreZo constitute the prototype in this case, but, generally speaking, the flexibility exists to use alternative, local models at different embayments to leverage previous validation efforts.

The predictive skill of the prototype is assessed with a base case of the regional model (CoSMoS) forcing a local model (BreZo) to simulate a historical and well-documented flood that occurred on January 10, 2005, because of an extreme high tide that overtopped the embayment defenses, *i.e.,* weir-like overtopping. Wave overtopping was not significant in this event, which makes it ideal for evaluating the local model. However, wave overtopping is important, in general, so simple modeling strategies to incorporate wave overtopping are examined. The study proceeds by considering several alternative parameterizations of the local model and forcing approaches to further examine data and model sensitivities. A previous study by Gallien, Schubert, and Sanders (2011) presented BreZo and its data requirements. Here, however, attention is turned to the regional–local model coupling needed to achieve forecasting capability. The study also characterizes uncertainties in local flood predictions that arise from the CoSMoS forcing, flood-defense data, topographic data, embayment bathymetric data, and the flood-mapping methodology, including simple strategies to account for wave overtopping. The successful regional–local coupling highlights the synergies achieved when regional and local modelers collaborate, as described here, as well as the potential pitfalls of extending regional models to the local level with limited local knowledge. The progress reported could serve as a paradigm for successful local and regional cooperation to improve flood preparedness and adaptation in a changing climate.

METHODS

Site Description

The City of Newport Beach, California, shown in Figure 1, is a densely populated, economically valuable, coastal community, located approximately 70 km southeast of Los Angeles, California. The city encompasses one of the largest estuarine embayments in California, Newport Bay, which is the terminus of the San Diego Creek watershed that extends 291 km^2 across central Orange County, California. The lower portion of the bay, Newport Harbor, is a pleasure-craft marina, where the shoreline is extensively hardened and defended from flooding by flood walls, whereas the upper portion of the bay includes extensive marshlands and a wildlife sanctuary. The city is geographically divided into three distinct terrain characterizations: (1) elevated marine terraces on the NW portion of the city, (2) high-relief elevations in the eastern section of the city, and (3) the urban, coastal lowlands bordering Newport Harbor, located in the city's central section, which is the geographical focus of this investigation. The peninsula that encloses the harbor is exposed to the Pacific Ocean on the S and W, from which, flood protection is provided by a sandy beach that dynamically adjusts in height and width with changes in wave and tide conditions and is subject to ongoing beach nourishment efforts. Balboa Island, California, lies within Newport Harbor and is one of the most densely populated communities in the United States. Concrete flood-defense walls constitute the primary flood protection mechanism for Balboa Island, California, and along the bay-side of the peninsula. Both Balboa Island and Balboa Peninsula, California, have suffered multiple seawater inundations in the past century, including the Hurricane Liza–generated swell in September 1968 and the El Niño storm events in 1972–73 and 1982–83, 1987–88, 1997–98, and 2005.

Flood Event and Validation Data Description

This study focuses on a flood event that occurred on January 10, 2005. The combination of an astronomical high tide and a low pressure system caused sea water inundation across both Balboa Peninsula and Balboa Island, California. The offshore swell was minimal (<1 m) and winds were mild (*ca*. 4 m/s); flooding was primarily the result of high embayment water levels that caused weir-like overtopping of the flood defenses (Gallien, Schubert, and Sanders, 2011).

Flooding was photodocumented by City of Newport Beach, California, employees and resulted in 85 digital photographs which, in combination with eyewitness accounts from City of Newport Beach, California, employees, provided essential data for model validation. The photographs consisted of 67 Balboa Peninsula, California, and 18 Balboa Island, California, flood scenes, which were examined for location, perspective, and wet–dry interfaces near identifiable features to determine water surface elevation. A selection of photographs may be seen in Gallien and Sanders (2012). Flood extent was manually mapped in ArcGIS (ESRI, Redlands, California) either directly

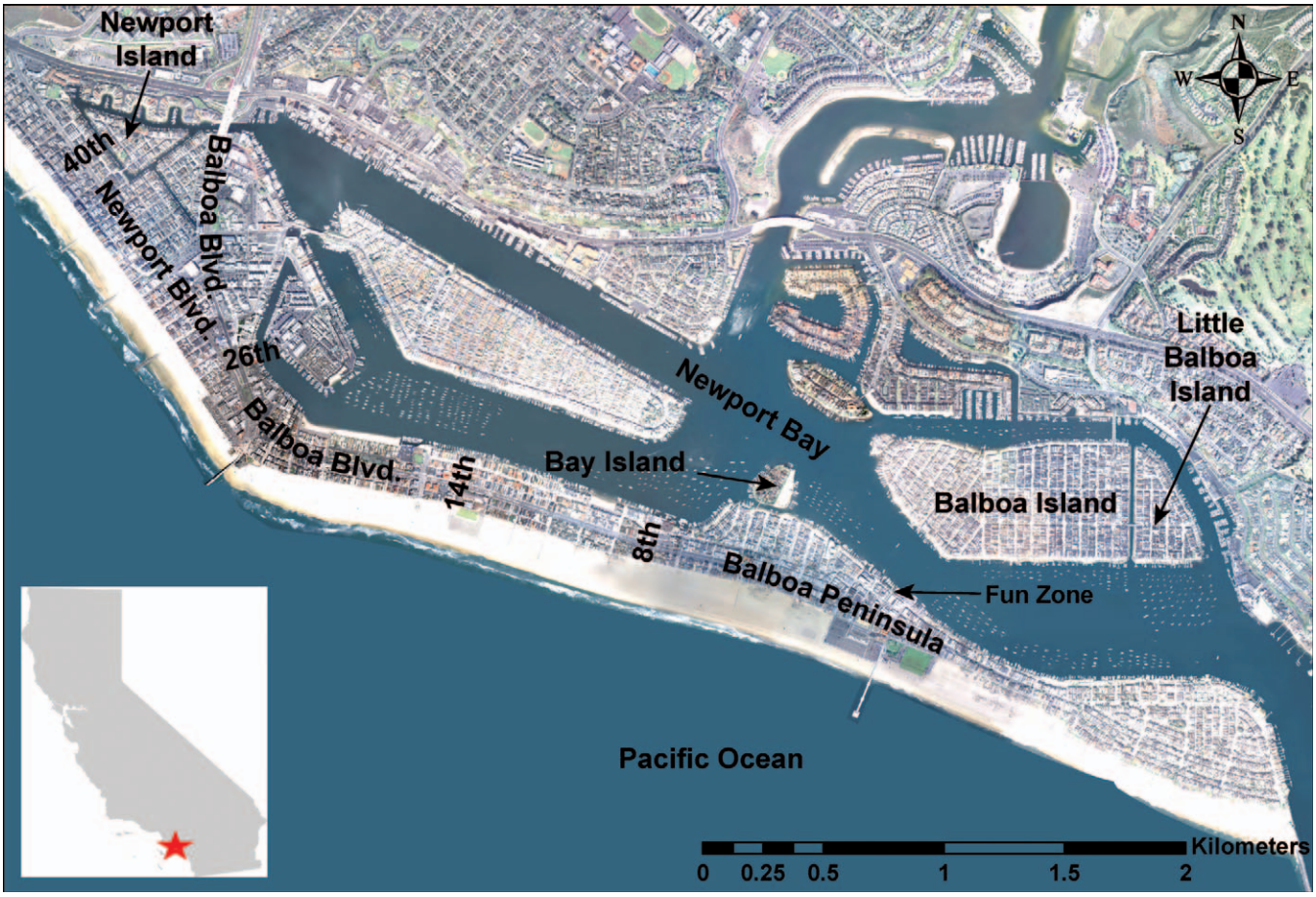

Figure 1. Newport Beach, California, study site. (Color for this figure is available in the online version of this paper).

from georeferenced photographic evidence or, if an area was not fully captured in the photos, by extrapolating these water levels to all hydraulically connected terrain at or below the determined elevation primarily using a raster DEM created from the raw LIDAR point cloud data and, in some cases, individual LIDAR point elevations as a guide. Eyewitness accounts were used in a similar manner to delineate flood zones SW of Newport Island, California, and S of Bay Island, California, where photodocumentation was unavailable. In this case, site-specific reports of flood extents served as the starting point for the manual extrapolation procedure. The resulting validation surface is limited to photographic reconstruction and, therefore, is subject to manually referenced errors in observed water level, for example, a 2–3 cm water level error may impart an areal-extent error of 3%–25% depending on the individual subregion. However, despite the inherent uncertainty in the observed water levels and consequently the individual sub-region flood extents, the flood validation surface correctly captures the spatial flooding patterns and is invaluable for highlighting differences between individual model outcomes.

Regional Ocean Modeling

CoSMoS is constructed as a nested modeling-train system (Barnard *et al.,* 2009), whereby global–regional 2-D WaveWatch3 (WW3) wave models are linked with regional–local 2-D Delft3D FLOW/SWAN models (Delft Hydraulics, 2007), and ultimately with one-dimensional (1D), cross-shore, surfzone-scale XBeach models (Roelvink *et al.,* 2009), spaced 100 m alongshore. In the Newport Beach, California, area, CoSMoS integrates three physical-process models and six layers of resolution, shown in Figure 2, stepping down from tens of kilometers to tens of meters. Swell was generated in the global and eastern North Pacific WW3 models by wind stress provided by the National Center for Environmental Prediction (NCEP) Global Forecasting System (GFS), a meteorological model tuned by ocean-basin–wide observations. Local–regional swell, seas, and surge were added into the Delft3D models using the wind and pressure fields from the NCEP North American Mesoscale (NAM) Forecasting System. Tidal boundary conditions for the regional Delft3D FLOW grid were obtained from the Oregon State University (OSU) TOPEX/Poseidon global-tide database (Egbert, Bennett, and Foreman, 1994). The time series of wave–spectral output and total water level at the 10-m

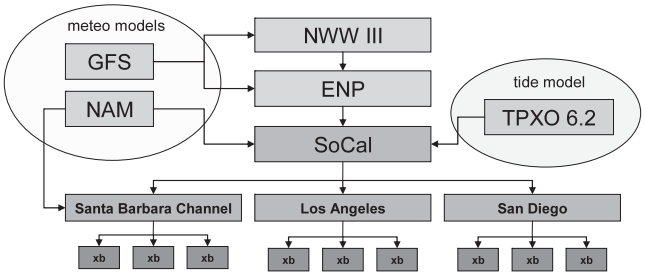

Figure 2. Coastal Storm Modeling System (CoSMoS) modeling framework.

bathymetric contour subsequently drove the sediment transport and shoreline-change module, XBeach, along 100-m alongshore-spaced, cross-shore profiles for the entire study area. XBeach simulates wave-group forcing and the subsequent infragravity motions within the surf zone, which dominate West Coast beaches during storms. XBeach is applied in one dimension to predict the cross-shore profile evolution, extreme run-up, and maximum water level along each cross-shore profile, assuming alongshore processes have minimal effect on local flooding and profile change during the short time frames of peak storm conditions, where large waves refract and approach the coast from a near-normal direction at most sites. Additionally, hindcasts of selected storms are accessible at http://cosmos.deltares.nl/SoCalCoastalHazards/index.html, and specific historical storms are available on request.

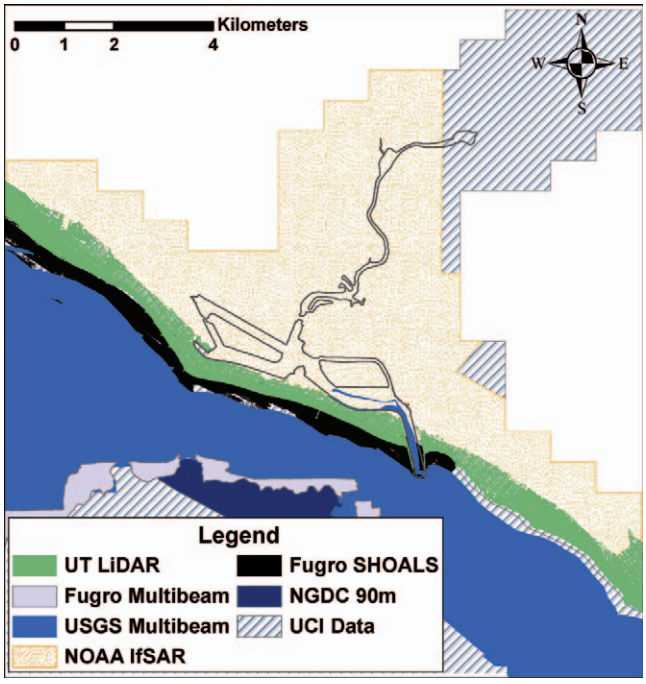

Figure 3. RDEM data sources. (Color for this figure is available in the online version of this paper).

Although the effects of wind and wave setup are considered, as well as (more important) barometric pressure, in the prediction of ocean heights, CoSMoS currently does not include any baroclinic effects (in particular, local upwelling and downwelling on the shelf and larger-scale water-level variations due to density effects), which also play an important role when it comes to predicting sea-surface heights. Strong downwelling events, for example, those preceding the 1997–98 El Niño, can easily add another 10–20 cm to the total water levels (Schwing *et al.,* 2002). These processes can be captured by using the 3D version of Delft3D at greater computational expense, and research is ongoing to understand the trade-offs between 2D and 3D modeling approaches along the California coast. Results of the 2D approach are reported here because this is how CoSMoS is presently configured to run for operational forecasting.

In Southern California, CoSMoS is supported by a 3-m resolution, bathymetric, and topographic DEM assembled from publically available data sets (Barnard and Hoover, 2010). We term this the *Regional DEM* or *RDEM*. Figure 3 shows the primary source data used by the RDEM in the Newport Harbor, California, region: topographic LIDAR, bathymetric LIDAR (*i.e.,* SHOALS), IfSAR data, and multibeam bathymetry data. The LIDAR and bathymetry data were used where possible; however, coverage was lacking in some regions (*e.g.,* Balboa Island, California, Little Balboa Island, California, limited portions of the peninsula), so those areas were filled using NOAA IfSAR data (http://www.csc.noaa.gov/digitalcoast/data/coastalifsar). The RDEM references all data to Universal Transverse Mercator (UTM) NAD83 Zone 11 North (horizontal) and NAVD88 (vertical). Data sources were merged using the ArcGIS mosaic application. For a complete discussion of the RDEM construction and metadata, please refer to Barnard and Hoover (2010).

CoSMoS was executed for the January 10, 2005, flood event in hindcast mode, and Figure 4 shows how the offshore water level prediction for Los Angeles compared with NOAA tide predictions and measurements at the Los Angeles tide gauge located 38 km NW of Newport Beach, California. This shows that CoSMoS captures a significant, nontidal offset (*ca*. 20 cm)

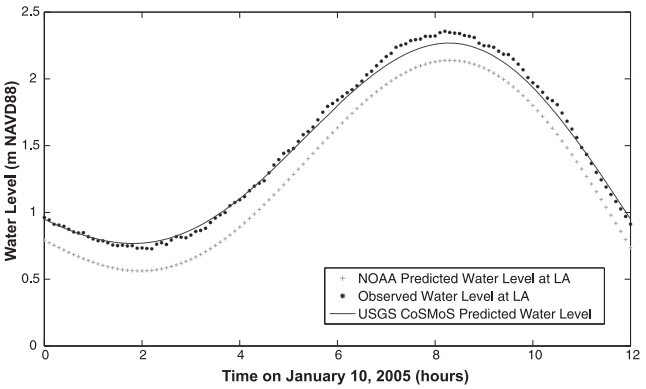

Figure 4. Water level comparison.

in the ocean level. Errors in the CoSMoS prediction were only about 1–2 cm for much of the falling and rising tide, although at the most critical time when the ocean height was at maximum, the error increases and CoSMoS underpredicts the maximum tide by 8.9 cm. Nevertheless, this represents a significant improvement over the NOAA astronomical-tide prediction. The NOAA astronomical-tide prediction underestimates the high-water level by 21.6 cm, compared with 8.9 cm underprediction with CoSMoS; the uncertainty of a critical forcing factor is reduced by more than 50%. This is considered particularly good considering that Delft 3D was run in a 2D mode.

Local Embayment Modeling

Literature points to the use of local embayment hydrodynamic models parameterized with high resolution digital terrain data to develop flood scenarios associated with sea level rise and storm event scenarios (Bates *et al.,* 2005; Brown, Spencer, and Moeller, 2007; Dawson *et al.,* 2009; Knowles, 2009; Poulter and Halpin 2008). Embayment models typically cover a domain that includes the embayment itself, coastal terrain vulnerable to flooding and open sea waters where boundary conditions are specified. The embayment is typically forced by an offshore water level and inland streamflow and/or runoff. In this case, the local embayment model was forced offshore by CoSMoS water-level data and at the head of the bay by streamflow corresponding to San Diego Creek. An approximate inflow rate of 0.35 m^3/s was used based on historical streamflow gauge data (USGS 11048500) from 1949–85 for the 2 months in which inundation was most likely to occur, December and January.

The local hydrodynamic model used in this study, BreZo, is a Godunov-type, finite-volume, 2D, shallow-water model with a robust wetting and drying algorithm for simulating tidal dynamics, streamflow, simple wall overtopping, and overland flow (Begnudelli and Sanders, 2006; Begnudelli, Sanders and Bradford, 2008). BreZo has been used extensively for river basin and dam-break flooding scenarios in both rural and urban settings (Begnudelli, Sanders, and Bradford, 2008; Gallegos, Schubert and Sanders 2012; Sanders, 2007, Sanders, Schubert, and Gallegos, 2008; Schubert and Sanders 2012; Schubert *et al.,* 2008). Similarly, 2D, Godunov-type codes have been successfully implemented in coastal embayment modeling (Arega and Sanders, 2004; Cea, French, and Vazquez-Cendon, 2006; Sanders, 2008), as well as urban-inundation modeling (Gallegos, Schubert, and Sanders, 2009; Sanders, Schubert, and Gallegos, 2008; Schubert and Sanders 2012; Schubert *et al.,* 2008; Villanueva and Wright, 2006), thus, providing an attractive candidate for simulating coastal-flooding events. A primary benefit of the Godunov-type scheme is the admission of flow discontinuities, such as abrupt elevation changes characteristic of flood defenses, streets, and curbs found in highly variable terrain inherent to a complex urban environment. An approximate Riemann-solver computes mass and momentum fluxes along the computation cell edges allowing transcritical flows that result from overtopping (Toro, 2001). Hence, weir-like overtopping flows are computed without any special tuning of the solver. The key issue is correctly setting the edge elevation to resolve the onset of weir-like overtopping.

BreZo uses an unstructured, triangular computational mesh and requires a combination of vertex and cell-based data to represent elevation and flow resistance, respectively. The domain encompasses all above and below water terrain around Newport Bay, California, and extends several kilometers offshore where a water-level boundary condition is enforced. For this study, the computational mesh consisted of approximately 500,000 computational cells ranging from the finest resolution (*ca*. 3.5 m) for the urbanized lowlands to a coarse resolution (*ca*. 300 m) for offshore and high-elevation areas. An intermediate resolution (*ca*. 25 m) was used for the bay and nearshore areas. Additional maximum area constraints were used to transition smoothly between the three primary resolutions. The mesh was generated using maximum cell area, minimum vertex angles, and edge position constraints in Triangle (Shewchuck, 1996). These constraints promote accuracy and computational efficiency, *e.g.,* a 30° minimum-angle constraint avoids stability problems that result from highly acute angles. Maximum cell areas were defined in areas of interest (urbanized lowlands) to resolve parcel-scale flooding, whereas offshore or high-elevations areas were assigned larger areas. Mesh vertices and edges were aligned with features that constrained overtopping, such as earthen embankments and flood defense walls, which facilitated accurate depiction of overtopping thresholds within the local hydrodynamic model. In some cases, very fine–scale curvature in flood walls forced localized mesh refinements well beyond the simulation resolution and, similar to Tsubaki and Fujita (2010), a manual smoothing procedure was used. Effectively, the flood wall was pushed slightly offshore (*ca*. $<$ 1m) to accommodate those fine features without degrading computational efficiency.

A Local Digital Terrain Model (LDTM) covering all simulation-domain bathymetry and topography was prepared from the best available local data to facilitate assignment of mesh vertex elevations. Source data included a 2006 city-commissioned LIDAR survey, bathymetric data for Newport Bay, California, obtained from 2003 and 2005, U.S. Army Corps of Engineers (USACE) surveys, and offshore bathymetry data retrieved from the National Geophysical Data Center Southern California Coastal Ocean Observing System (SCCOOS). Imagery was provided at 7.62-cm resolution but coarsened to 30 cm to facilitate data management. The entirety of the LIDAR survey consisted of 53.5 million surface samples covering 146 km^2 in 262 tiles. Only 112 tiles represented geographical areas of interest, and therefore, the remaining tiles were discarded, yielding an average LIDAR point density of 0.185 points/m^2 with a vertical accuracy of 0.182 m root mean square error (RMSE). All LIDAR data were reported in NAD1983 California State Plane Zone VI (feet) and NAVD88 feet. Upper and Lower Bay USACE bathymetric data were reported in NAVD88 and corresponded to 1-m and 3-m resolutions, respectively. Offshore SCOOS bathymetry data were available at 3 arc-second resolution (*ca*. 100 m) and were specified in mean lower low water (MLLW) which, in Newport Beach, California, differs from NAVD88 by 5.5 cm. Given that offshore bathymetry data corresponded to depths greater than 10 m, the relative error ($\Delta z/h$, normalized by depth) was less than 1% and was inconsequential for flooding analysis. Prior testing revealed that a 5.5-cm offshore bathymetry difference affected maxi-

mum water levels by less than 0.05 cm, and therefore, no datum correction was made in this particular instance. The LTDM data sources are shown in Figure 5 and consisted of approximately 12 million points. These points were merged into a single point file using NAD83 and NAVD88 datums and interpolated using an eight-point, inverse-distance weighting function in ArcGIS to create a 3-m DTM in a Cartesian (raster) format.

The LIDAR returns on flood defense structures were minimal; therefore, publicly accessible flood barriers, such as sea walls, wharves, and earthen embankments, were surveyed using a Magellan ProMark3 Real-Time Kinematic Global Positioning System (RTK-GPS) and Orange County Real-Time Network Base Station corrections yielding *ca*. 1-cm vertical RMSE accuracy. Although these survey data were not included in the LDTM, flood thresholds were enforced in the computational mesh by aligning cell edges with flood defense walls along the peninsula and Balboa, California, and Little Balboa Island, California, mesh elevations were assigned directly from the RTK-GPS survey data. This promotes accurate prediction of weir-like overtopping flows. In addition to vertex elevations, the local hydrodynamic model requires flow-resistance parameterization. Although not addressed in this particular article, testing revealed flow-resistance parameterization effects on flood extent were negligible within a range of physically realistic values, and therefore, a uniform resistance parameter representative of flow across a natural surface ($n = 0.025$ $m^{-1/3}$ s) was used for all hydrodynamic simulations. Note that the terminology LDTM is used here (instead of LDEM) because all elevation data correspond to ground heights. In contrast, RDEM heights may correspond to vegetation canopy or roof tops depending on the source data.

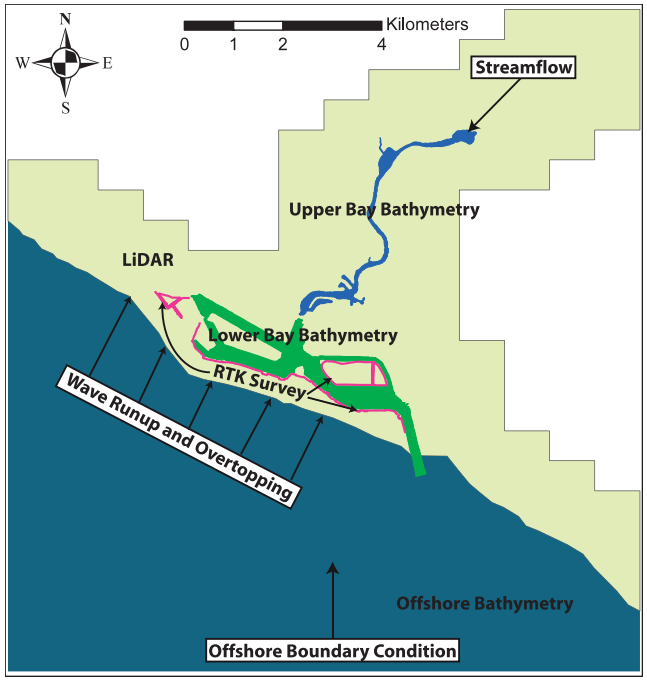

Figure 5. LDTM data sources and forcing. (Color for this figure is available in the online version of this paper).

RDEM and LDTM Differences

Elevation differences between the RDEM and LDTM are shown graphically in Figure 6 to frame the flood modeling results that follow. Here, red colors indicate areas of higher RDEM elevations (surface model), and blue depicts areas where the RDEM elevations are lower. Differences between random selections of points from the DEMs are also shown in Table 1. This shows that, along the peninsula, where LIDAR data were used in both elevation models, the road surfaces are in excellent agreement as shown by similar mean elevations and minimum, maximum, and standard deviations. However, the RDEM terrain appears to contain some roof returns, and that is evidenced by the maximum elevation, which is more than 3 m above the LDTM. Balboa Island, California, exhibits significant differences between the two DEMs. There, RDEM mean elevations were significantly higher for both road surfaces and random points, which can be explained by IfSAR returns detecting tree canopy and building rooftops (Sanders, 2007). That is further supported by a random sampling of buildings, which indicates that the mean elevation is greater than 3 m higher in the RDEM than it is in the LDTM. Prior research has shown flood models perform poorly when elevation corresponds to tree tops or surface objects instead of bare earth because vegetated areas may incorrectly block flow instead of resisting flow (Sanders, 2007).

Substantial differences in bay bathymetry are also observed and highlight a significant hazard of using regional data for local hydrodynamic modeling; the mean elevation difference between the RDEM and LDTM is nearly 5 m. The RDEM depicts the elevation of the bay at 1.056 m NAVD88, well above MLLW. This discrepancy was attributed to the IfSAR data used

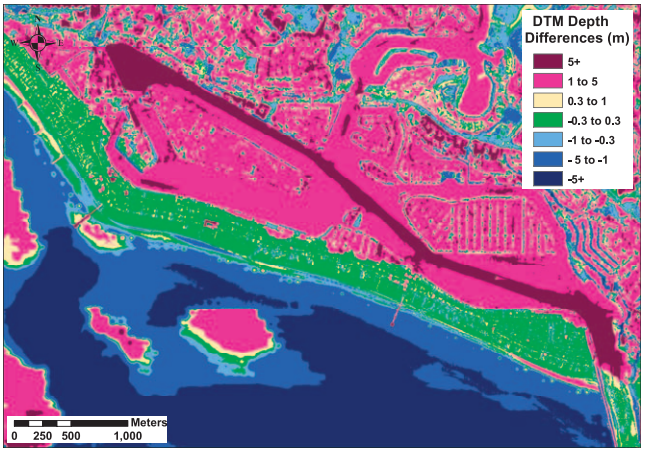

Figure 6. Elevation differences between LDTM and RDEM. (Color for this figure is available in the online version of this paper).

Table 1. *Digital elevation model differences.*

Feature	*n* Points	Terrain	Data Source	z_{mean} (m)	σ (m)	z_{min} (m)	z_{max} (m)
Peninsula	117	LDTM	2006 Newport Beach LIDAR (bare earth)	3.041	0.775	1.727	5.860
		RDEM	LIDAR 2007, LIDAR 2005, NOAA IfSAR	3.280	1.138	1.584	8.633
Peninsula roads	57	LDTM	2006 Newport Beach LIDAR (bare earth)	2.640	0.566	1.976	4.093
		RDEM	LIDAR 2007, LIDAR 2005, NOAA IfSAR	2.682	0.595	1.958	4.026
Balboa Island	115	LDTM	2006 LIDAR (bare earth)	2.128	0.207	1.683	2.692
		RDEM	LIDAR 2007, LIDAR 2005, NOAA IfSAR	4.891	1.513	1.808	9.615
Balboa roads	53	LDTM	2006 LIDAR (bare earth)	1.886	0.152	1.572	2.196
		RDEM	LIDAR 2007, LIDAR 2005, NOAA IfSAR	3.315	1.104	1.540	6.566
Structures (piers, buildings, bridges)	57	LDTM	2006 Newport Beach LIDAR (bare earth)	1.729	2.193	−4.300	3.869
		RDEM	LIDAR 2007, LIDAR 2005, NOAA IfSAR	4.998	2.794	1.110	13.233
Lower bay	69	LDTM	2003 and 2005 USACE	−3.745	1.201	−7.337	−2.318
		RDEM	LIDAR 2007, LIDAR 2005, NOAA IfSAR	1.056	0.957	−6.751	1.250
Offshore	127	LDTM	3 arc-second NGDC coastal relief Model	−24.436	32.503	−203.124	−2.224
		RDEM	2008 Multibeam and 1996, 1998, 1999 USGS	−30.513	33.830	−201.818	−2.278

to resolve the area containing the bay and likely represented elevation data filled from neighboring land measurements. Offshore, the RDEM and LDTM generally agree on minimum and maximum values. However, the average elevation of the LDTM is 6 m above that of the RDEM. In this case, the RDEM is more accurate. The RDEM data were a recent, high-resolution, 2-m multibeam bathymetry survey, whereas the LDTM employed coarser, 3 arc-second resolution bathymetric data, which poorly resolved the deep submarine canyon immediately offshore of Newport Beach, California, resulting in the positive elevation bias.

Prototype Forecasting System and Variants

CoSMoS system is capable of providing a 3 day forecast of ocean heights every 12 hours (Barnard *et al*., 2009), and a parallel version of BreZo is capable of executing a 12-hour simulation of flood embayment inundation with parcel-scale resolution in less than an hour (Sanders, Schubert, and Detwiler, 2010). Hence, the prototype forecasting system has the potential to support a 3-day horizon with a 12-hour refresh, as currently supported by CoSMoS. In this study, however, the prototype modeling system was also implemented in hindcast mode for the documented January 10, 2005, flood event to assess predictive skill and modeling sensitivities. The BreZo simulation covered a period of 12 hours and started approximately 8 hours before the peak tide. By resolving the ebb–flood–ebb cycle, BreZo captured the amplification of the tide within Newport Bay, California, from the excitation of higher-order modes, the overtopping of defenses at high tide, and the overland flow along streets into low-lying areas.

A base case was used to assess the predictive skill of the prototype, and several variants (alternative parameterizations and modeling approaches) were used to examine the data and model sensitivities. The base case involved CoSMoS parameterized with the RDEM as described in Barnard and Hoover (2010), and the local hydrodynamic model, BreZo, was parameterized with the LDTM, as described in Gallien, Schubert, and Sanders (2011). Variants included (1) external forcing from alternative water levels, including NOAA tide predictions and Los Angeles tide-gauge measurements; (2) simulations with and without streamflow forcing along with the substitution of the RDEM into the local model instead of the LDTM to understand the effects of topographic and bathymetric errors; and (3) use of a PSP model, instead of the hydrodynamic model for flood-zone delineation.

The PSP method is popular for regional sea-level rise assessment and is straightforward to implement in geographical information system (GIS) software (*e.g.,* Heberger *et al.,* 2009; Poulter and Halpin, 2008; Strauss *et al.,* 2012). The PSP model, implemented here (and in CoSMoS) used a maximum shoreline water level projected along each XBeach transect (spaced *ca*. 100 m apart). Bordering cells at, or lower than, the maximum water level were subsequently flooded based on eight-way connectivity (Poulter and Halpin, 2008). Hence, the model checks for hydraulic connectivity according to height data in the DEM and is, therefore, reliant on DEM resolution and quality. PSP models perform well in settings where the embayment water level is sustained for a timescale that is long compared with the timescale of overland flow, allowing time for offshore and backshore water levels to equilibrate (Gallien, Schubert, and Sanders, 2011). In urban areas protected by flood walls that are exceeded for a matter of minutes to hours, as is common in Southern California, that assumption is not appropriate, and the interest here was in understanding the magnitude of the resulting bias.

Performance Metrics

Predictive skill is measured using four fit metrics that consider the coherence between the observed and predicted flood zone, and uncertainty in predictions arising from data sources and process models are measured by changes in those fit measures. First, an agreement fit measure, F_A, is defined as the intersection of predicted and observed flood extent, divided by the union of observed and predicted flood extent,

$$F_A = \frac{E_P \cap E_O}{E_P \cup E_O} \tag{1}$$

where E_P and E_O represent the predicted and observed flood extents, respectively. A fit measure of unity corresponds to identical prediction and observation, whereas a fit measure of zero corresponds to no agreement between the prediction and observation. This metric is known as the *Coefficient of Areal Correspondence* (Taylor, 1977), and in flood-modeling practice, this metric may be referred to as $F<1>$ and is generally

Table 2. *January 10, 2005 simulation results.*

Figure	Terrain	DEM Resolution (m)	Offshore Water Level (m)	Maximum Water Level (m)	Embayment Model	Wall?	Streamflow?	Flooded Area (km^2)	F_A	F_{UP}	F_{OP}	F_{AO}
7a	LDTM	3	2.267	2.330	Hydrodynamic	Yes	Yes	0.085	0.1970	0.4592	0.3438	0.3002
7b	LDTM	3	2.137	2.155	Hydrodynamic	Yes	Yes	0.006	0.0006	0.9467	0.0527	0.0007
7c	LDTM	3	2.356	2.402	Hydrodynamic	Yes	Yes	0.311	0.2148	0.0879	0.6973	0.7096
8a	LDTM	3	2.267	2.315	Hydrodynamic	No	Yes	0.932	0.0962	0.0128	0.8910	0.8828
8b	LDTM	3	2.267	2.283	Hydrodynamic	No	No	0.836	0.1002	0.0207	0.8791	0.8289
8c	RDEM	3	2.267	2.411	Hydrodynamic	No	Yes	1.364	0.0462	0.0274	0.9264	0.6273
8d	RDEM	3	2.267	1.856	Hydrodynamic	No	No	0.016	0.0036	0.8625	0.1339	0.0042
9a	RDEM	3	2.267	2.267	—	No	No	0.110	0.1996	0.3798	0.4206	0.3445
9b	LDTM	3	2.267	2.267	—	No	No	0.716	0.1368	0.0063	0.8569	0.9563
9c	RDEM	3	2.267	3.590	—	No	No	0.868	0.0590	0.0537	0.8873	0.5233
9d	LDTM	3	2.267	3.590	—	No	No	1.771	0.0582	0.0001	0.9417	0.9983

recommended for both deterministic and uncertain calibration because it considers underprediction and overprediction equally undesirable (Schumann *et al.,* 2009). Second, a measure of underprediction, F_{UP}, characterizes the portion of flooded area observed but not predicted as follows:

$$F_{UP} = \frac{E_P - E_P \cap E_O}{E_P \cup E_O} \tag{2}$$

and, in this case, a fit measure zero represented no underpredictions, and values near one represent near-total underprediction. Third, a measure of overprediction, F_{OP}, characterizes the portion of the flooded area predicted, but not observed, as follows:

$$F_{OP} = \frac{E_O - E_P \cap E_O}{E_P \cup E_O} \tag{3}$$

where a fit measure of near zero represents no overprediction, and fit measures near unity represent nearly total overprediction. Finally, F_{AO} represents the fraction of the observed flood that was correctly predicted and is described as,

$$F_{AO} = \frac{E_P \cap E_O}{E_O} \tag{4}$$

where a fit measure of one would represent complete prediction success. This metric is attractive when overprediction is strongly preferable to modeling underprediction and, therefore, generally favors models that predict larger flooded areas.

In flood-prediction efforts, both underprediction and overprediction are undesirable. Optimizing the fit agreement, F_A is a priority; however, many planners consider underprediction unacceptable and, therefore, would weight F_{AO} heavily. The best models will maximize F_A and F_{AO} simultaneously.

RESULTS

A total of eleven January 10, 2005, storm-event simulations, shown in Table 2 and Figures 7–9, are presented to validate the prototype modeling system (CoSMoS + BreZo) and to examine its sensitivity to data and model components. Each scenario is evaluated based on its prediction of flood extent using the previously defined performance metrics. Figure 7a corresponds to the prototype modeling system, and all other results (Figures 7b and c, 8a–d, and 9a–d) correspond to variants that are designed to reveal important model sensitivities.

Attention is focused first on the effects of offshore forcing: Figure 7a corresponds to forcing by CoSMoS water-level prediction for the site, Figure 7b corresponds to forcing by the NOAA tide prediction for the Newport Harbor entrance, and Figure 7c corresponds to forcing by NOAA tide measurements at Los Angeles, California. Figure 7a shows the prototype modeling system achieves a relatively high fit agreement of $F_A = 0.1970$ (compared with all other scenarios) and a moderate level of underprediction, $F_{UP} = 0.4592$. By comparison, the NOAA tide-prediction forcing (Figure 7b) yields no significant flooding reflected by a near-zero fit agreement and a substantially increased level of underprediction, $F_{UP} = 0.9467$. This is explained by the 13-cm difference between the height of the predicted tide and the higher CoSMoS prediction, which accounts for more atmospheric and oceanic processes. When BreZo is forced with historical water level measurements from the Los Angeles, California, tide gauge (Figure 7c), 8.9 cm higher than the predicted CoSMoS water level, total flooded area increases significantly to 0.311 km^2, fit agreement increases slightly to $F_A = 0.2148$ compared with CoSMoS case (Figure 7a), and underprediction drops substantially to 0.0879. A large area of underprediction near 14th Street and several small areas along the northwestern portion of Balboa Boulevard are observed in all three models. This contributes to the relatively low fit scores (compared with other studies) and is attributed to subsurface (storm sewer) flows that are not resolved by the model but which act to redistribute flood water across the site. Areas of overprediction shown on Balboa Island, California, near 26th Street and on the peninsula near Bay Island, California, may also be affected by the omission of sewers. Sewer pipes can store a fraction of the flood volume that overtops defenses. If this storage effect were incorporated into the model, a reduction in flooded area would be expected.

These results show that the most accurate prediction is achieved with measurements of the ocean water level, but recognizing that this is not available *a-priori,* the CoSMoS prediction holds considerable promise by reducing water-level uncertainty by more than 50% compared with the NOAA tide prediction. Moreover, these results highlight the sensitivity of flood predictions to small perturbations in offshore forcing (*ca.* 10 cm).

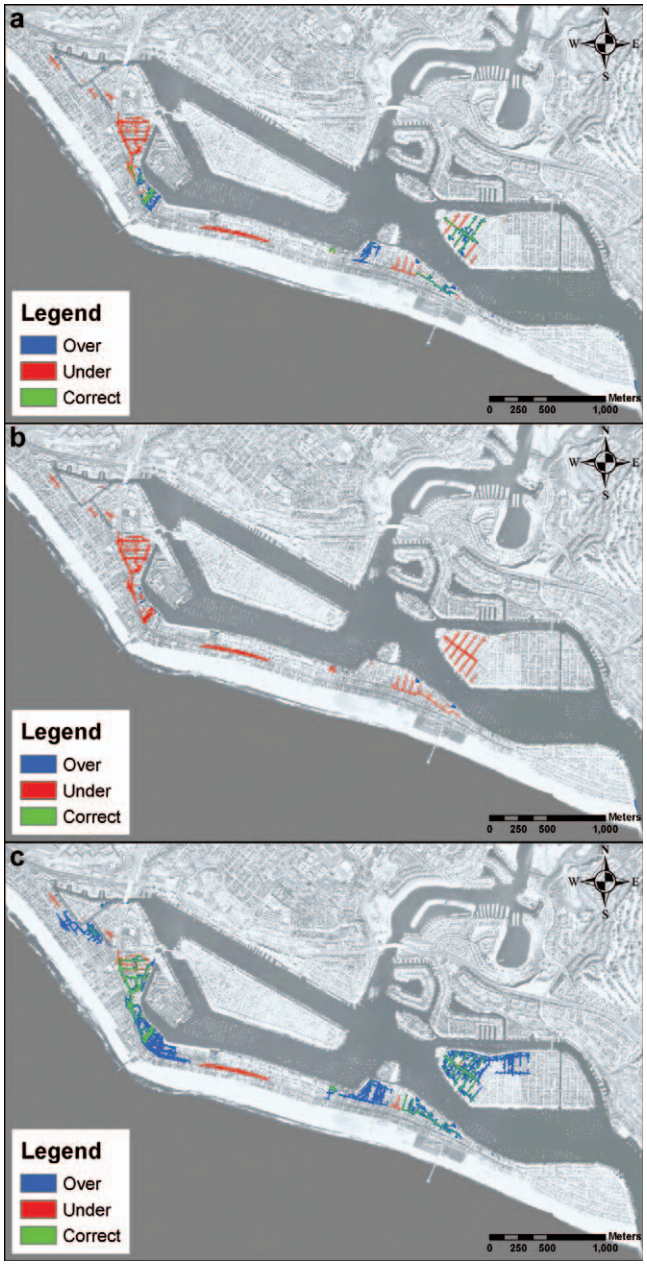

Figure 7. Water level boundary condition results for (a) CoSMoS, (b) NOAA tide prediction, and (c) Los Angeles historical tide gauge data. (Color for this figure is available in the online version of this paper).

With evidence that the regional CoSMoS model and the local BreZo model can be coupled to provide parcel-scale flood predictions in a forecasting mode and, hence, validation of the prototype, attention turns to the sensitivity of the modeling system to the data and models used to support it. The second set of simulations shown in Figure 8 focus on the effects of the DEM (LDTM *vs*. RDEM) and streamflow forcing (included *vs*. not included) on BreZo predictions of flood inundation. In this case, wall survey data are not considered, so the overall flood zones are larger than they are in Figure 7 (as one would expect) and more sensitive to elevation differences, which is of particular interest. Figures 8a and b correspond to predictions using the LDTM with and without streamflow, respectively, whereas Figures 8c and 8d correspond to predictions using the RDEM with and without consideration of streamflow, respectively.

A comparison of Figures 8a and b, where the LDTM is used to consider the effects of streamflow, show only minimal differences in predicted flooding. However, when the RDEM data are substituted for the LDTM, Figures 8c and d, significant changes in both spatial pattern and flood prediction are observed. The RDEM predictions are extremely sensitive to streamflow. This is explained by the very shallow bay depths defined by the RDEM (Figure 6; Table 2), in contrast to the LDTM, which affords several meters of depth to convey flood water through the bay.

Figures 8b and d reveal the sensitivity of flooding predictions to the DEM when there is no streamflow forcing, and only ocean water level forcing is considered. Generally, less flooding is predicted using the RDEM compared with the LDTM. The RDEM leads to a prediction where overprediction is minimal ($F_{OP} = 0.1339$), and underprediction dominates ($F_{UP} = 0.8625$). In contrast, the LDTM gives a prediction where overprediction is dominant ($F_{OP} = 0.8791$), and underprediction is minimal ($F_{UP} = 0.0207$).

Underprediction of flooding on Balboa Island, California, is expected with the RDEM because elevations here are based on IfSAR data that overestimate terrain heights by several meters (Table 1). On the other hand, extensive overprediction on Balboa Peninsula, California, is somewhat surprising because the elevations compare favorably here (Figure 6; Table 1). This overprediction is attributed to the unrealistically shallow bay bathymetry depicted by the RDEM. Shallow embayment depths magnify the effects of streamflow on flooding because the cross-sectional area of the bay is restricted. Collectively, the preceding results show that the bias of the RDEM toward very shallow embayment depths acts to increase the flooding sensitivity to streamflow and decrease the flooding sensitivity to high ocean levels.

The third set of results in Figure 9 focuses on the PSP or *bathtub* flood-mapping approach. Figures 9a and b shows the PSP prediction using CoSMoS water-level data and the RDEM and LDTM, respectively. Flooded area significantly increases from 0.110 km^2 to 0.716 km^2 using the LDTM method instead of the RDEM system, and underprediction is substantially reduced, from $F_{UP} = 0.3798$ to $F_{UP} = 0.0063$. A decrease in fit agreement F_A is observed because of the overprediction associated with using the LDTM. However, LDTM performance appears to be superior to RDEM based on the fraction of observed flooding correctly predicted F_{AO}, which represents a nearly perfect score ($F_{AO} = 0.9567$ *vs*. 0.3445). Generally, the migration from surface data to bare earth data yields a significantly larger flooded area and may improve accuracy by limiting underprediction.

Analysis thus far has focused on flooding caused by weir-like overtopping of flood defenses. However, wave overtopping represents another important driver of coastal flooding, which has, historically, contributed to flooding at Newport Beach,

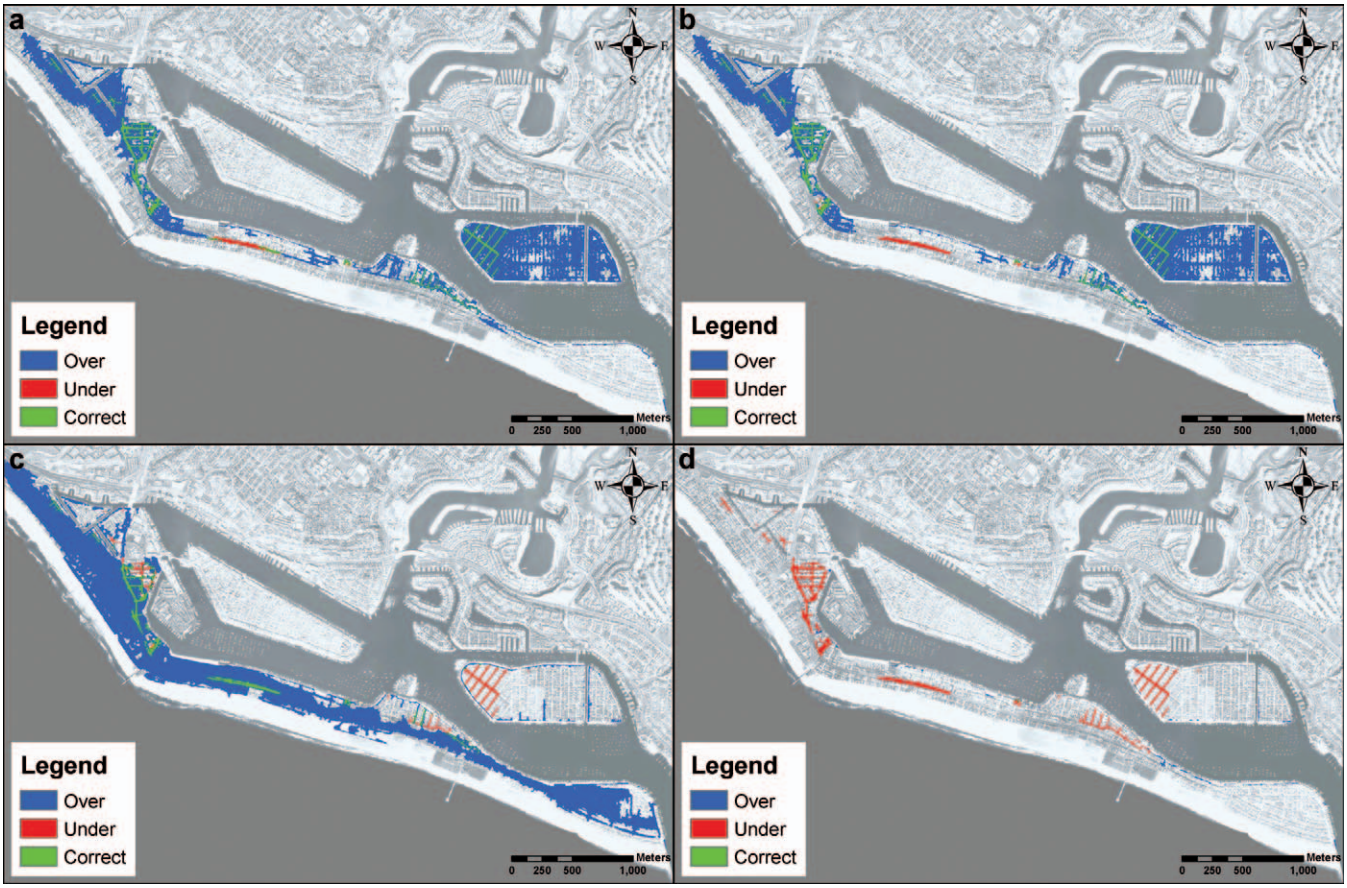

Figure 8. (a) LDTM with streamflow, (b) LDTM without streamflow, (c) RDEM with streamflow and (d) RDEM without streamflow. (Color for this figure is available in the online version of this paper).

California. CoSMoS predicts wave run-up at each of the XBeach transects, and previous work has suggested that PSP methods be used to account for wave-driven flooding with a "total water level" that represents the sum of the predicted water levels and the run-up (*e.g.,* FEMA, 2004; Heberger *et al.,* 2009). Figures 9c and d show PSP flood predictions with the RDEM and LDTM, respectively, based on the total water level. The RDEM case (Figure 9c) reveals poor spatial patterns of flooding, areas of significant overprediction (peninsula) and underprediction (Balboa Island, California,) and low total fit agreement ($F_{AO} = 0.5233$), whereas the LDTM case suffers from overprediction and consequently yields a lower fit agreement F_A. Once again, the LDTM case gives a high score based on the fraction of observed flooding correctly predicted ($F_{AO} = 0.9983$) because it is biased toward overprediction of flood extent.

DISCUSSION

Three primary issues have been identified for effective parcel-scale, urbanized, embayment flood forecasting: an accurate water level characterization to predict the onset and rate of overtopping, models that account for both weir-like overtopping and wave overtopping mechanisms, and highly accurate local data to parameterize and validate models.

A time series of water level offshore of an embayment represents critical input to a local hydrodynamic model, and uncertainty in embayment water levels is linked to the description of tides, surges, and sea level rise. (Here, surge refers to not only storm effects but other processes that contribute to the nontide residual.) For a given hydrodynamic scenario, the offshore water level may be determined from NOAA tidal predictions, a water level forecast that incorporates surge or, if the scenario is a hindcast, from local historical data. In this study, historical data performed most accurately, however, the CoSMoS prediction of water level provided significant benefit over the astronomical tide prediction, reducing water level uncertainty by more than 50% and is strongly recommended for future flood-prediction scenarios. Moreover, in regions where climatic factors (*e.g.,* El Niño) super-elevate coastal water levels, CoSMoS would offer superior water level forecasts compared with the *a priori* NOAA astronomical predictions.

Overtopping flows represent key processes in urbanized coastal flood forecasting that has been noted in previous studies

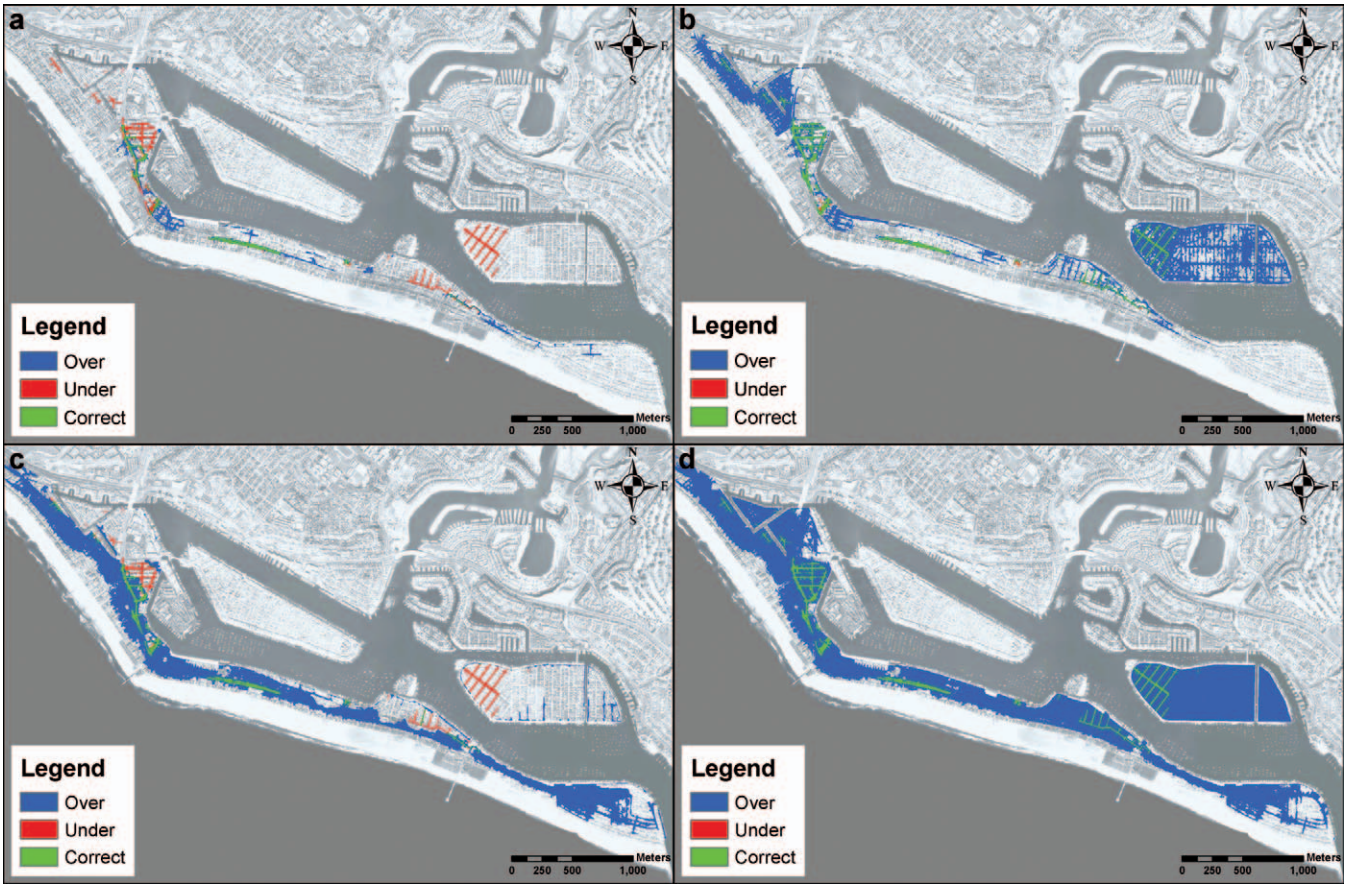

Figure 9. Raster modeling results for CoSMoS hindcast water level with (a) RDEM, (b) LDTM, and with wave run-up for (c) RDEM and (d) LDTM. (Color for this figure is available in the online version of this paper).

(*e.g.,* Brown, Spencer, and Moeller, 2007; Coulton *et al.,* 2002; Hunt, 2005). The fundamental issue is that, within defended urbanized lowlands, flood extent is constrained by the volume of water that penetrates flood defenses from a combination of weir-like and wave overtopping flows. Weir-like overtopping flows appear to be scaled well in the local model. This results from explicit resolution of flood walls in the computational mesh and use of a Riemann solver to compute overtopping flows. However, this approach is not designed to account for wave overtopping. Work here shows that PSP methods are biased by overprediction in defended lowlands and use of a total water level only exacerbates the error. Hence, future research needs to advance overtopping models with the ability to account for dynamic and spatially distributed wave-overtopping flows.

Local data resolution encompasses multiple issues: DTM resolution, bathymetry, streamflow, and flood threshold representation. The IfSAR data used for a portion of the RDEM resulted in a digital surface model depicting vegetation and rooflines that is unacceptable for urban flood modeling because of high elevation bias and the inability to resolve fine-scale features that constrain or convey flow. Furthermore, embayment bathymetry represents a critical issue; accurate bathymetry data are needed to resolve important local processes, such as tidal amplification, which affects water level, and the routing of terrestrial flood events through the embayment. The unrealistically shallow bathymetry associated with the RDEM acted to attenuate the predicted effects of tidal flooding and exacerbate the predicted effects of terrestrial flooding when used in the context of the hydrodynamic model. This resulted in very poor spatial flooding patterns and the lowest ranked fit agreements of all the CoSMoS forced-hydrodynamic simulations. Using the RDEM, the hydrodynamic model predicted a flooded area was 85 times greater than the zero streamflow forecast. In addition, on Balboa Island, California, the hydrodynamic model performed reasonably well (compared with LDTM predictions) for the wrong reason: the effects of an overpredicted embayment water height (resulting from inaccurate bathymetry data) was negated by unrealistically high terrain heights (from IfSAR data). Hence, two significant errors counteracted each other relative to predicting the flood extent. This research highlights the importance of parameterizing coastal flooding models not only with the best available local data but also with data that meets certain accuracy standards.

For bathymetry data, this is likely to correspond to a relative error based the depth, but results here do not offer a specific tolerance. Finally, if regional model output is used to forecast coastal flooding through a PSP model, exploitation of the locally parameterized LDTM significantly improves overall prediction and minimizes underprediction.

Previous research has suggested coastal flooding is most severe at shoreline reaches protected by structures such as walls, wharves, and embankments (Coulton *et al.,* 2002) and that these structures are often poorly mapped by remote-sensing systems such as topographic LIDAR (Gallien, Schubert, and Sanders, 2011; Webster *et al.,* 2004). Gallien, Schubert, and Sanders (2011) show that a *ca* 1-cm RMSE RTK-GPS survey is sufficient for resolving flooding defense-barrier elevations and that inclusion of these structures in hydrodynamic models is essential to accurate flood prediction (Gallien, Schubert, and Sanders, 2011). Breaching can also be important (*e.g.,* Battjes and Gerritsen 2002; Brown, Spencer, and Moeller, 2007; Morris and Hassan, 2002). Further improvement in predictive skill beyond that achieved here would require scrutiny of both public and privately owned flood defenses, including a comprehensive inspection of infrastructure condition, including cracks, gaps, and leakage during high-water conditions. Additionally, the role of storm sewers relative to back-flooding, storage, and redistribution should be considered.

Finally, this study benefitted from a unique validation data set, which would make the site an excellent candidate for an operational flood-forecasting system. Generally, high-quality validation data are rare, which fundamentally obstructs efforts to advance predictive modeling. Therefore, in anticipation of higher sea levels, improved monitoring of urban flood events should be a priority (Anselme *et al.,* 2011; Bates *et al.,* 2005; Gallien, Schubert, and Sanders, 2011; Poulter and Halpin, 2008, Smith, Bates, and Hayes, 2012).

CONCLUSIONS

This study demonstrates the potential to forecast urban coastal flooding at the parcel-scale by using a publicly available multiscale model, CoSMoS, to force a local hydrodynamic model that explicitly resolves embayment tide dynamics, overtopping flows that penetrate flood defenses, and overland flow along the road network. The regional model is critical to account for important nontidal processes (*e.g.,* winds, waves, surge) that contribute to flood events in addition to accounting for tides. The importance of local data is emphasized, including flood defense heights, land surface topography, embayment bathymetry, and local sewer properties. An important benefit of the proposed regional–local modeling coupling is that responsibility for local model parameterization and validation can be managed at the local level, whereas responsibility for regional-scale processes (winds, waves, tides, *etc*.) can be managed at a regional level.

Poor predictive skill results from using less-accurate regional data in local models and omitting key local data, such as flood defense heights. In urbanized embayments, regional data that significantly underestimates the embayment depth may cause local model predictions to be overly sensitive to streamflow and to attenuate the effects of high ocean levels. Also, use of IfSAR data to model the land surface height negatively biases the prediction of flooded area because that sensor technology poorly captures bare earth heights when vegetation and buildings are present. Therefore, bare earth DTMs, augmented with a comprehensive flood-defense survey, are strongly recommended over DEMs (which may reflect buildings or vegetation heights) because of the need to properly resolve features that channel (*i.e.,* roadways) and constrain (*i.e.,* walls, embankments) flow.

Urbanized lowlands are susceptible to flooding from weir-like overtopping of defenses and wave overtopping of defenses and beaches. Weir-like overtopping is resolved here within the local hydrodynamic model, but wave overtopping is more complex. The PSP methods, based on total water level (water level plus run-up), overpredict flood extent in defended terrain and, in a significant wave storm, exclusion of run-up would likely underpredict flooding on the open coast. To significantly advance coastal flood prediction, there is a need for new methods that resolve dynamic and spatially-distributed overtopping flows within the context of an urban coastal flood prediction model.

The condition of flood defenses (*e.g.,* cracks, leaks, gaps) can affect the overtopping volume in ways that are not easily modeled, and sewers act to redistribute flood water. Hence, the condition and configuration of infrastructure represents an additional source of uncertainty in flood predictions. Although assessment and failure probability for a given event is outside the scope of this study, they represent another important dimension of flood forecasting and deserve further investigation.

ACKNOWLEDGMENTS

This work was supported by grants from the National Science Foundation (CMMI-0825165 and CMMI-1129730) and made possible by the gracious cooperation of the City of Newport Beach, California, personnel who shared geospatial data, photographs, and invaluable site-specific knowledge. The authors gratefully acknowledge the anonymous reviewers for their constructive comments on the draft manuscript.

LITERATURE CITED

Arega, F. and Sanders, B.F., 2004. Dispersion model for tidal wetlands. *Journal of Hydraulic Engineering,* 130(8), 739–754.

Anselme, B.; Durand, P.; Thomas, Y., and Nicolae-Lerma, A., 2011. Storm extreme levels and coastal flood hazards: a parametric approach on the French coast of Langunedoc (district of Leucate). *Comptes Rendus Geoscience,* 343, 677–690.

Barnard, P.L; O'Reilly, B.; van Ormondt, M.; Elias, E.; Ruggiero, P.; Erikson, L.H.; Hapke, C.; Collins, B.D.; Guza, R.T.; Adams, P.N., and Thomas, J.T., 2009. *The Framework of a Coastal Hazards Model: A Tool for Predicting the Impact of Severe Storms*. Santa Cruz, California: U.S. Geological Survey Open-File Report 2009-1073, 19p.

Barnard, P.L. and Hoover, D., 2010. *A Seamless, High-Resolution, Coastal Digital Elevation Model (DEM) for Southern California*. Reston, Virginia: U.S. Geological Survey Data Series, DS-487, 8p.

Bates, P.D.; Dawson, R.J.; Hall, J.W.; Horritt, M.S.; Nicholls, R.J.; Wicks, J., and Hassan, M.A.A.M., 2005. Simplified two-dimensional numerical modelling of coastal flooding and example applications. *Coastal Engineering,* 52(9), 793–810.

Battjes, J.A. and Gerritsen, H., 2002. Coastal modeling for flood defense. *Philosophical Transactions of the Royal Society A,* 360, 1461–1475.

Begnudelli, L. and Sanders, B.F., 2006. Unstructured grid finite volume algorithm for shallow after transport with wetting and drying. *Journal Hydraulic Engineering,* 132(4), 371–84.

Begnudelli, L.; Sanders, B.F., and Bradford, S.F., 2008. Adaptive Godunov-based model for flood simulation. *Journal of Hydraulic Engineering,* 134(6), 714–725.

Bromirski, P.D.; Miller, A.J.; Flick, R.E., and Auad, G., 2011. Dynamical suppression of sea level rise along the Pacific Coast of North America: Indications for imminent acceleration. *Journal of Geophysical Research-Oceans,* 116, C07005.

Brown, J.D.; Spencer, T., and Moeller, I., 2007. Modeling storm surge flooding of an urban area with particular reference to modeling uncertainties: a case study of Canvey Island, United Kingdom. *Water Resources Research,* 43(W06402).

Bunya, S.; Dietrich, J.C.; Westerlink, J.J.; Ebersole, B.A.; Smith, J.M.; Atkinson, J.H.; Jensen, R.; Resio, D.T.; Luettich, R.A.; Dawson, C.; Cardone, V.J.; Cox, A.T.; Powell, M.D.; Westerlink, H.H., and Roberts, H.J., 2010. A high-resolution coupled riverine flow, tide, wind, wind wave and storm surge model for southern Louisiana and Mississippi, part I: model development and validation. *Monthly Weather Review,* 138(2), 345–377.

Cayan, D.; Tyree, M.; Dettinger, M.; Hidalgo, H.; Das, T.; Maurer, E.; Bromirski, P.; Graham, N., and Flick, R., 2009. *Climate Change Scenarios and Sea Level Rise Estimates for the California 2008 Climate Change Scenarios Assessment*. Sacramento: California Climate Change Center, 62p.

Cea, L.; French, J.R., and Vazquez-Cendon, M.E., 2006. Numerical modelling of tidal flows in complex estuaries including turbulence: an unstructured finite volume solver and experimental validation. *International Journal of Numerical Methods in Engineering,* 67, 1909–1932.

Coulton, K.G.; Battalio, B.; Garrity, N.; Chandrasekera, C., and Cooper, P., 2001. Coastal flood studies in the Puget Sound, Washington State, U.S.A. *In:* Ewing, L. and Wallendorf, L. (eds.). *Proceedings of Solutions to Coastal Disasters '02* (San Diego, California, ASCE), pp. 267–281.

Crowell, M.; Coulton, K.; Johnson, C.; Wescott, J.; Bellmo, D.; Edelman, S., and Hirsch, E., 2010. An estimate of the U.S. population living in the 100-year coastal flood hazard areas. *Journal of Coastal Research,* 26(2), 201–211.

Dawson, R.J.; Dickson, M.E.; Nicholls, R.J.; Hall, J.W.; Walkden, M.J.A.; Stansby, P.; Mokrech, M.; Richards, J.; Zhou, J.; Milligan, J.; Jordan, A.; Pearson, S.; Rees, J.; Bates, P.; Koukoulas, S., and Watkinson, A., 2009. Integrated analysis of risks of coastal flooding and cliff erosion under scenarios of long term change. *Climatic Change,* 95(1–2), 249–288.

Delft Hydraulics. 2007. *User Manual Delft3D-FLOW: WL| Delft Hydraulics*. Delft, The Netherlands: Delft Hydraulics, 614p.

Egbert, G.; Bennett, A., and Foreman, M., 1994. TOPEX/Poseidon tides estimated using a global inverse model. *Journal of Geophysical Research–Oceans,* 99, C12, 24, 821–24, 852.

European Commission. *A new EU floods directive: directive 2007/60/EC*. http://ec.europa.eu/environment/water/flood_risk/index.htm.

FEMA (Federal Emergency Management Agency). 2004. Guidelines and specifications for flood hazard mapping partners appendix D. *Final Draft Guidelines for Coastal Flood Hazard Analysis and Mapping for the Pacific Coast of the United States*. http://www.fema.gov/library/viewRecord.do?id=2188.

Flick, R.E.; Murray, J.F., and Ewing, L.E., 2003. Trends in United States tidal datum statistics and tide range. *Journal of Waterway, Port, Coastal and Ocean Engineering,* 129(4), 155–164.

Gallegos, H.A.; Schubert, J.E., and Sanders, B.F., 2009. Two-dimensional, high-resolution modeling of urban dam-break flooding: a case study of Baldwin Hills, California. *Advances in Water Resources,* 32, 1323–1335.

Gallegos, H.A.; Schubert, J.E., and Sanders, B.F., 2012. Structural damage prediction in a high-velocity dam-break flood: a field-scale assessment of predictive skill. *Journal of Engineering Mechanics,* doi: 10.1061/(ASCE)EM.1943–7889.0000427.

Gallien, T.W.; Schubert, J.E., and Sanders, B.F., 2011. Predicting tidal flooding of urbanized embayments: a modeling framework and data requirements. *Coastal Engineering,* 58(6), 567–577.

Gallien, T.W. and Sanders, B.F., 2012. An integrated high resolution urban coastal flood model. *In: Headwaters to Oceans 2012*. San Diego, California: California Coastal Coalition. http://www.coastalconference.org/h20_2012/presentations/2012-05-31-Thursday/Session%209A%20-%20Climate%20Change%20Adaptation/Gallien-Urban%20Coastal%20Flood%20Modeling.pdf.

Hanson, S.; Nicholls, R.; Ranger, N.; Hallegatte, S.; Corfee-Morlot, J.; Herweijer, C., and Chateau, J., 2011. A global ranking of port cities with high exposure to climate extremes. *Climatic Change,* 104, 89–111.

Hasselmann, S.; Hasselmann, K.; Bauer, E.; Janssen, P.A.E.M.; Komen, G.J.; Bertotti, L.; Lionello, P.; Guillaume, A.; Cardone, V.V.; Greenwood, J.A.; Reistad, M.; Zambresky, L., and Ewing, J.A., 1988. The WAM model—a third generation ocean wave prediction model. *Journal of Physical Oceanography,* 18, 1775–1810.

Heberger, M.; Cooley, H.; Herrera, P.; Gleick, P.H., and Moore, E., 2009. *The Impacts of Sea-Level Rise on the California Coast*. Sacramento: California Climate Change Center, 115p.

Holthuijsen, L.H.; Booij, N., and Ris, R.C., 1993. A spectral wave model for the coastal zone. *In:* Magoon, O.T. and Hemsley, J.M. (eds.). *Proceedings of the 2nd International Symposium on Ocean Wave Measurement and Analysis* (New Orleans, Louisiana, ASCE), pp. 630–641.

Hunt, J.C.R., 2005. Inland and coastal flooding: developments in prediction and prevention. *Philosophical Transactions of the Royal Society–A,* 363, 1475–1491.

Jelenianski, C.P.; Chen, J., and Shaffer, W.A., 1992. SLOSH: *Sea Lake and Overland Surges from Hurricanes*. Washington, DC: National Oceanic and Atmospheric Administration Technical Report NWS 48, 71p.

Jevrejeva, S.; Moore, J.C., and Grinsted, A., 2012. Sea level projections to AD2500 with a new generation of climate change scenarios. *Global and Planetary Change,* 80–81, 14–20.

Knowles, N., 2009. Potential inundation due to rising sea levels in the San Francisco Bay Region. *San Francisco Estuary and Watershed Science,* 8(1), 1–19.

MMC (Multihazard Mitigation Council). 2005. *Natural Hazard Mitigation Saves: An Independent Study to Assess the Future Savings from Mitigation Activities*. Washington, DC: National Institute of Building Science. 168p.

Morris, M.W. and Hassan, M., 2002. Breach formation through embankment dams and flood defense embankments: a state of the art review. Wallingford, UK: H.R. Wallingford, 21p.

Mulligan, R.P.; Perrier, W.; Toulany, B.; Smith, P.C.; Hay, A.E., and Bowen, A.J., 2011. Performance of Nowcast and forecast wave models for Lunburg Bay, Nova Scotia. *Atmosphere-Ocean,* 49(1), 1–7.

Néelz, S.; Pender, G.; Villaneuva, I.; Wilson, M.; Wright, N.G.; Bates, P.; Mason, D., and Whitlow, C., 2006. Using remotely sensed data to support flood modelling. *Water Management,* 159, 35–43.

Nicholls, R.J., 2011. Planning for the impacts of sea level rise. *Oceanography,* 24(2), 144–157.

O'Reilly, W.C. and Guza, R.T., 1993. A comparison of spectral wave models in the Southern California Bight. *Coastal Engineering,* 19(3), 263–282.

O'Reilly, W.C.; Seymour, R.J.; Guza, R.T., and Castel, D., 1993. Wave monitoring in the Southern California Bight. *In:* Magoon, O.T. and Hemsley, J.M. (eds.). *Proceedings of the 2nd International Symposium on Ocean Wave Measurement and Analysis*. (New Orleans, Louisiana, ASCE), pp. 849–863.

Padilla-Hernandez, R.; Perrie, W.; Toulany, B., and Smith, P.V., 2007. Modeling of two northwest Atlantic storms with third-generation wave models. *Weather and Forecasting,* 22, 1229–1242.

Poulter, B. and Halpin, P.N., 2008. Raster modelling of coastal flooding from sea-level rise. *International Journal of Geographical Information Science,* 22(2), 167–182.

Roelvink, D.; Reniers, A.; Van Dongeren, A.; van Thiel de Vries, J.; McCall, R., and Lescinski, J., 2009. Modelling storm impacts on

beaches, dunes and barrier islands. *Coastal Engineering*, 56, 1133–1152.
Sanders, B.F., 2007. Evaluation of on-line DEMs for flood inundation modeling. *Advances in Water Resources,* 30(8), 1831–1843.
Sanders, B.F., 2008. Integration of a shallow-water model with a local time step. *Journal of Hydraulic Research,* 46(8), 466–475.
Sanders, B.F.; Schubert, J.E., and Gallegos, H.A., 2008. Integral formulation of shallow-water equations with anisotropic porosity for urban flood modeling. *Journal of Hydrology,* 362, 19–38.
Sanders, B.F.; Schubert, J.E., and Detwiler, R.L., 2010. A parallel, unstructured grid, Godunov-type, shallow-water code for high-resolution flood inundation modeling at the regional scale. *Advances in Water Resources,* 33, 1456–1467.
Schubert, J.E. and Sanders, B.F., 2012. Building treatments for flood inundation models and implications for predictive skill and modeling efficiency. *Advances in Water Resources,* 41, 49–64.
Schubert, J.E.; Sanders, B.F.; Smith, M.J., and Wright, N.G., 2008. Unstructured mesh generation and landcover-based resistance for hydrodynamic modeling of urban flooding. *Advances in Water Resources,* 31, 1603–1621.
Schumann, G.; Bates, P.D.; Horritt, M.S.; Matgen, P., and Pappenberger, F., 2009. Progress in integration of remote sensing—derived flood extent and stage data and hydraulic models. *Review of Geophysics,* 47, 1–20.
Schwing, F.B.; Murphree, T.; deWitt, L., and Green, P.M., 2002. The evolution of oceanic and atmospheric anomalies in the northeast Pacific during the El Niño and La Niña events of 1995–2001. *Progress in Oceanography,* 54, 459–491.
Sheng, Y.P.; Alymov, V., and Paramygin, V.A., 2010. Simulation of storm surge, wave, currents and inundation in the Outer Banks and Chesapeake Bay during Hurricane Isabel in 2003: The importance of waves. *Journal of Geophysical Research,* 115, 1–27.
Sheng, Y.P.; Zhang, Y., and Paramygin, V.A., 2010. Simulation of storm surge, wave and coastal inundation in the Northeastern Gulf of Mexico region during Hurricane Ivan in 2004. *Ocean Modelling,* 35, 314–331.
Shewchuk, J.R., 1996. Triangle: engineering a 2D quality mesh generator and Delaunay triangulator in applied computational geometry: towards geometric engineering. *In:* Lin, M.C. and Manocha, D. (eds), *Lecture Notes in Computer Science,* Volume 1148. Berlin: Springer, pp. 203–222.
Smith, D.I., 1994. Flood damage estimation—a review of urban stage-damage curves and loss functions. *Water Resources of South Africa,* 20(3), 231–238.
Smith, R.A.E.; Bates, P.D., and Hayes, C., 2012. Evaluation of a coastal flood inundation model using hard and soft data. *Environmental Modelling & Software,* 30, 35–46.
Strauss, B.H.; Ziemlinski, R.; Weiss, J.L., and Overpeck, J.T., 2012. Tidally adjusted estimates of topographic vulnerability to sea level rise and flooding for the contiguous United States. *Environmental Research Letters,* 7, 014033. doi: 10.1088/1748–9326/7/1/014033, 12p.
Taylor, P.J., 1977. *Quantitative Methods in Geography: An Introduction to Spatial Analysis*. Boston: Houghton Mifflin Harcourt, 396p.
Tebaldi, C.; Strauss, B.H., and Zervas, C.E., 2012. Modelling sea level rise impacts on storm surges along US coasts. *Environmental Research Letters,* 7, 014032. doi:10.1088/1748–9326/7/1/014032, 11p.
Tolman, H.L., 1997. *User Manual and System Documentation of WAVEWATCH-III* version 1.15. Camp Springs, Maryland: NOAA/NWS/NCEP/OMB Technical Note 151. 97p.
Toro, E.F., 2001. *Shock-Capturing Methods for Free-Surface Shallow Flows*. Chichester, UK: Wiley, 309p.
Tsubaki, R. and Fujita, I., 2010. Unstructured grid generation using LIDAR data for urban flood inundation modeling. *Hydrological Processes,* 24, 1404–1420.
Vermeer, M. and Rahmstorf, S., 2009. Global sea level linked to global temperature. *Proceedings of the National Academy of Sciences,* 106 (51), 21527–21532.
Villanueva, I. and Wright, N.G., 2006. Linking Riemann and storage cell methods for flood predictions. *In: Proceedings of the ICE—Water Management,* 159(1), 27–33.
Webster, T.L.; Forbes, D.L.; Dickie, S., and Shreenan, R., 2004. Flood-risk mapping for storm-surge events and sea-level rise using lidar for southeast New Brunswick. *Canadian Journal of Remote Sensing,* 32(3), 194–211.